OAK RIDGE NATIONAL LABORATORY
OPERATED BY
UNION CARBIDE CORPORATION
NUCLEAR DIVISION
POST OFFICE BOX X
OAK RIDGE, TENNESSEE 37830

ORNL/MIT-245

DATE: December 21, 1976

SUBJECT: Three-Dimensional Temperature History of a Multipass Filled Weldment, Part 2

Authors: J.A. Pinkowish and P.K. Whitman

Consultant: J.F. King

ABSTRACT

Computer simulation of the three-dimensional temperature history in a multipass filled weldment was attempted by modifying a transient heat transfer code, HEATING5. The model includes temperature dependent physical parameters, radiation and convection heat losses, turbulent and laminar convection in the molten pool, and variable arc velocity, intensity, and weld geometry. The model requires approximately 28 CPU min to simulate one second of welding.

Oak Ridge Station
School of Chemical Engineering Practice
Massachusetts Institute of Technology
W.M. Ayers, Director

Contents

1. SUMMARY

HEATING5, a computer program designed to solve transient heat transfer problems, was used to predict the three-dimensional temperature profiles of a multipass filled weldment. This was accomplished by defining a weldment geometry for the multipass profiles, inputting a moving, symmetric heat flux which travels at finite steps along the weld, developing tabular functions to describe the temperature dependent material properties and heat transfer coefficients, locating the maximum stable time increment for the solution procedure, and generating temperature profiles for up to 0.55 cm along the weld groove.

The major conclusion of this project is that HEATING5 could be used to solve for the desired temperature profiles, but substantial work is still necessary to refine the simulation and decrease CPU time. The recommendations for refining the program center on determining the optimum time step and grid spacing and predicting the shape and properties of the molten pool.

2. INTRODUCTION

2.1 Background

Welding two pieces of metal often subjects the materials to extremely high temperatures and cooling rates. While extremely rapid cooling rates will leave residual stresses and strains in the metal, slower cooling can heat temper the effected metal and leave the weldment stronger than the original metal. In addition, the types and concentrations of the crystals composing a particular piece of metal are determined by the temperature history of the metal; the magnitude of the maximum temperature and the length of time the metal remains above a critical temperature where phase transformations can occur (730°C for most low-carbon steels) are of greatest importance. The crystalline structures present in the metal then determine many of its thermal and mechanical properties including its specific heat, conductivity, tensile strength, ductility, and hardness. In joining two thick pieces of metal, it is necessary to cut away part of the adjacent metal and fill the resultant groove with several passes of the arc, adding molten filler metal with each pass. One common configuration is the V-butt, shown in Fig. 1. Since some areas of the weldment are heated several times during the welding process, it is desired to develop an accurate method to predict the temperature profiles developed during welding and hence allow prediction of the strength of the multipass weldment.

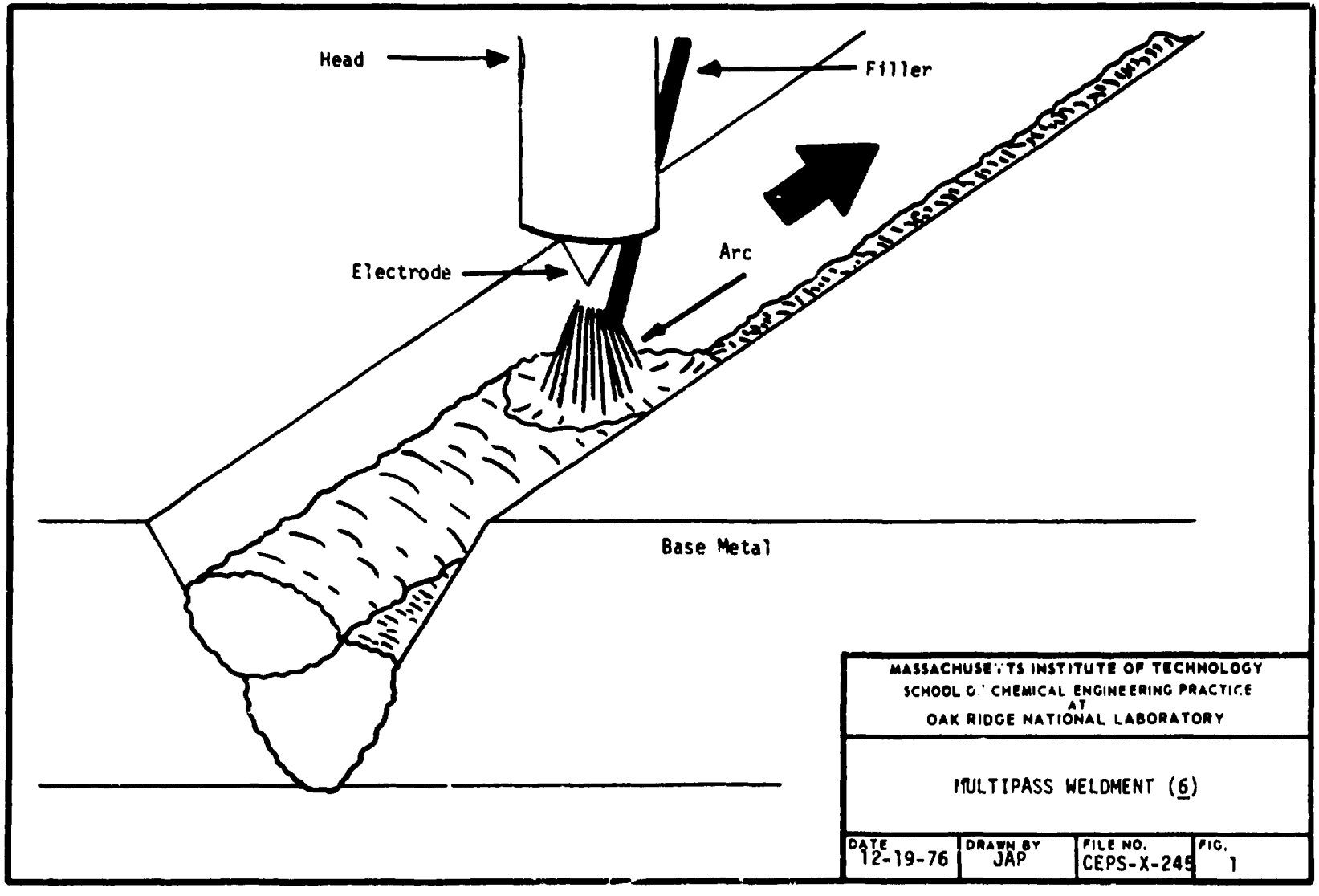
Head
Filler
Electrode
Arc
Base Metal
MASSACHUSETTS INSTITUTE OF TECHNOLOGY
SCHOOL OF CHEMICAL ENGINEERING PRACTICE
AT
OAK RIDGE NATIONAL LABORATORY
MULTIPASS WELDMENT (6)
DATE 12-19-76
DRAWN BY JAP
FILE NO. CEPS-X-245
FIG. 1

2.2 Previous Work

Analytical solutions to the governing equations for heat flow have been derived for two-dimensional models (thin plates) by assuming constant material properties and either a point or line heat source and by ignoring heat losses to the environment (14, 15, 17). While these solutions correlate well with the experimental isotherms that are far from the weld head, there are significant limitations to the analytical predictions close to the weld head or for more complicated geometrics.

Computer programs (10, 11, 12, 17) have been developed to numerically solve the partial differential equations describing two or three-dimensional heat flow in welds. However, since none of these programs include temperature dependent material properties, radiative and convective heat losses, and realistic methods for inputting the heat generated by the welding arc all in the same program, a previous MIT group (6) combined the salient points of the existing models and developed an approach to determine the three-dimensional temperature history of a multipass weldment.

2.3 Scope of the Project

The goal of this project was to develop a computer program to predict the three-dimensional temperature history of a multipass, filled weldment. This objective was achieved by translating a conceptual model of the welding process, presented by Kleinschmidt *et al.* (6), into a model which could be simulated by HEATING5 (16), a computer program capable of solving the finite difference equations describing transient, three-dimensional heat flow with phase changes.

3. COMPUTER SIMULATION

3.1 Physical Model

In multipass welding of two thick steel plates, a V-butt is formed to ensure that some base metal will fuse with the filler metal at every point in the juncture (Fig. 1). The computer model simulates multipass V-butt welding of two 304 SS plates by a tungsten-inert gas (TIG) welding arc operated by a welding machine.

The welding process occurs as follows. Before each pass begins, the two steel plates are preheated to 121°C. The welding arc then travels the length of the groove at 0.21 - 0.42 cm/sec, fusing approximately 0.15-gm base metal for each 1.00-gm filler metal. An electric arc (9.5 V, 155 amp) transfers heat to the metal directly below it by two mechanisms: (1) the collision of electrons with the metal surface, the principle

mechanism, and (2) forced convection from the hot plasma produced by resistance heating in the air gap between the weld head and the metal plate (6, 9, 12). Argon gas surrounds the hot plasma and effectively shields the remainder of the plate from it. Joule heating through the plates was found to be negligible (12).

For an observer traveling with the electrode, a quasi-steady state temperature profile develops in the metal around the electrode; i.e., the positions of the isotherms in the weldment remain constant with respect to the welding head (6, 17). A heat affected zone (HAZ), defined as the region within the 730°C isotherm, approximately 1-2-cm wide, develops. Inside the HAZ the metal is above the critical temperature for crystal phase changes. The HAZ is analyzed by three regions (see Fig. 2): (1) a turbulent molten pool directly under the arc, (2) a laminar molten pool behind the turbulent pool, and (3) a solid metal zone at elevated temperatures. The turbulent pool is assumed to be isothermal because a variety of forces such as Lorentz mixing, uneven arc pressure, and the arc plasma impinging on the surface keep it well-mixed (1, 6, 8). The laminar region has slow natural convection currents (2).

3.2 Computer Implementation

3.2.1 Geometry of the Weldment

The geometry of the weldment was simulated in the computer model by a series of rectangular regions (see Fig. 3). The weld extended the length of the V-groove and had a square cross-section with each side 0.3175 cm. The filling order of the V-groove was adopted from Kleinschmidt *et al.* (6). The V-groove cross-section was simulated by four rectangular sections, each 0.3175-cm high and 0.1588-cm wide. The region boundaries shown in Fig. 4 were selected according to the specifications detailed in Sect. 8.1.1. There were six possible applicable boundary conditions for the surface faces of each region (see Fig. 3): (1) natural convection and radiation from a horizontal plate hot side up, (2) natural convection and radiation from a horizontal plate hot side down, (3) natural convection and radiation from vertical surfaces not in the V-groove, (4) convection and radiation for a horizontal face on the V-groove, (5) convection and radiation for a vertical face on the V-groove, and (6) heat flux into the region under the arc with no convection and radiation. When no boundary condition was specified, conduction with the adjacent metal was assumed.

3.2.2 Assumptions for the Model

In actual welding practice, the filler metal and base metal compositions are not identical. However, it was determined that property differences between the base metal and the filler metal for the application are negligible (6). In the computer simulation the filler metal was assumed to already be in place in the weld groove (as solid base metal) before the pass was begun. Hence, filler metal not under the arc was preheated by

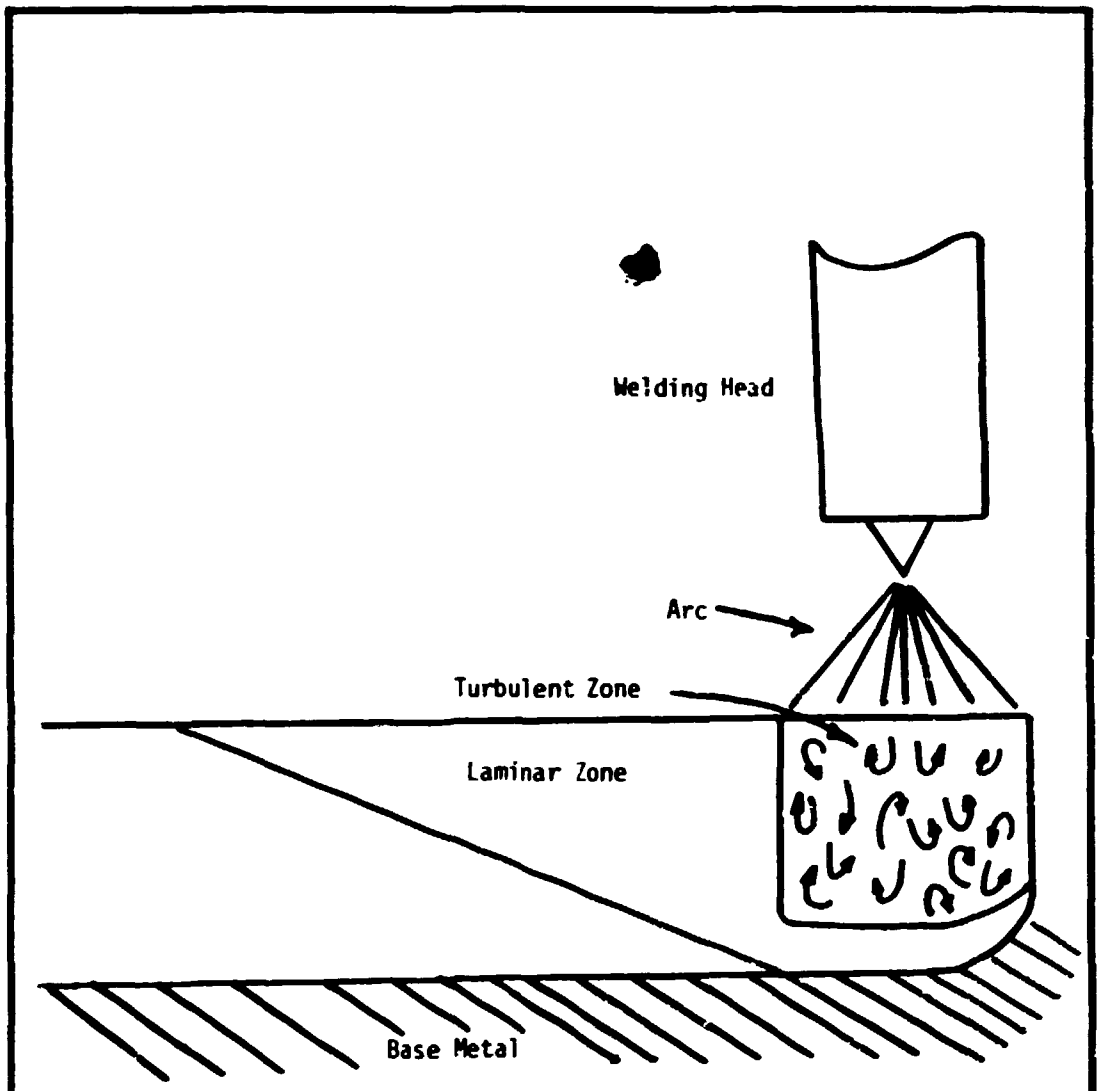

MASSACHUSETTS INSTITUTE OF TECHNOLOGY
SCHOOL OF CHEMICAL ENGINEERING PRACTICE
AT
OAK RIDGE NATIONAL LABORATORY

SIDE VIEW OF THE HEAT AFFECTED ZONE (6)

DATE	DRAWN BY	FILE NO.	FIG.
12-19-76	JAP	CEPS-X-245	2

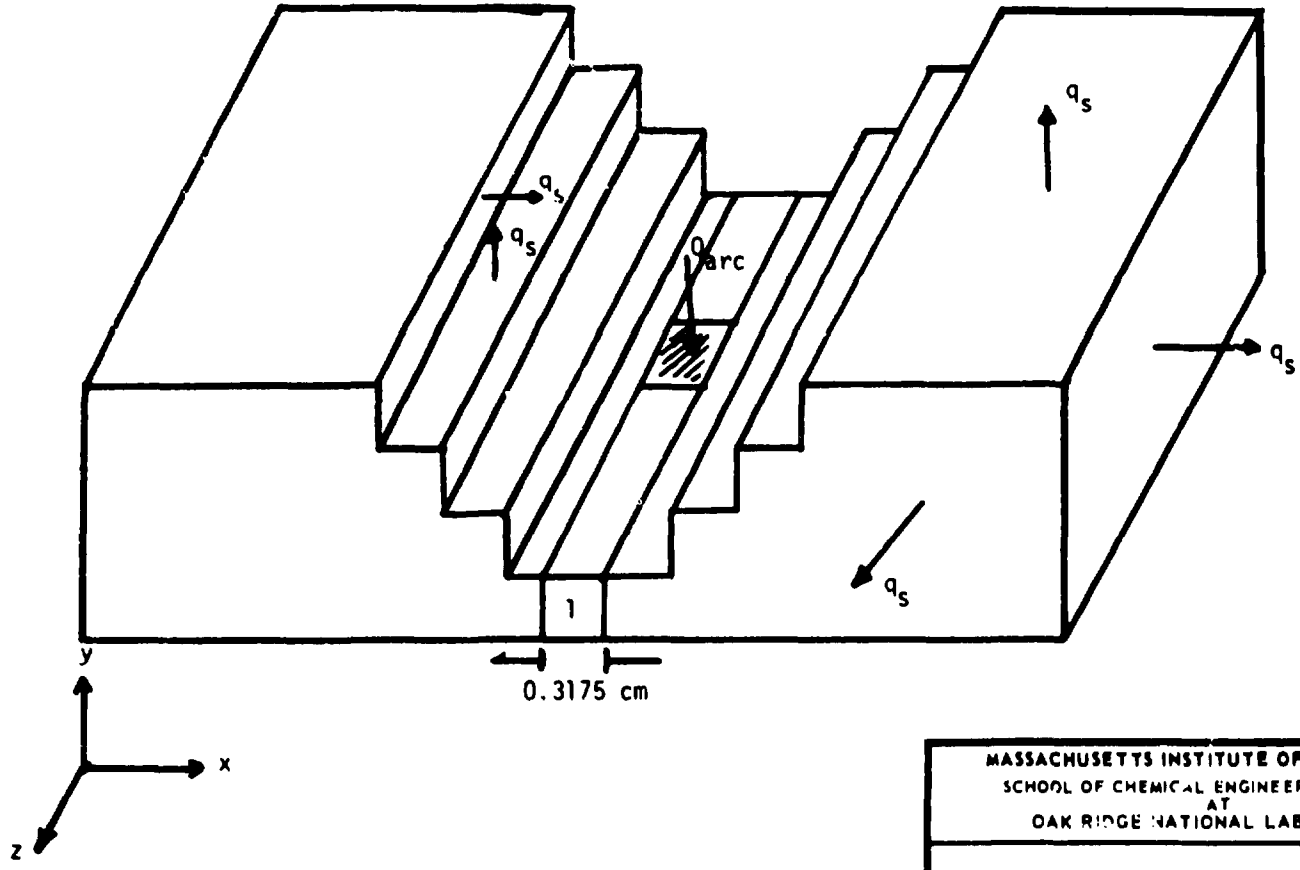

MASSACHUSETTS INSTITUTE OF TECHNOLOGY
SCHOOL OF CHEMICAL ENGINEERING PRACTICE
AT
OAK RIDGE NATIONAL LABORATORY

APPROXIMATION OF V-BUTT WELD
FOR COMPUTER SIMULATION

DATE	DRAWN BY	FILE NO.	FIG.
12-19-76	PKW	CEPS-X-245	3

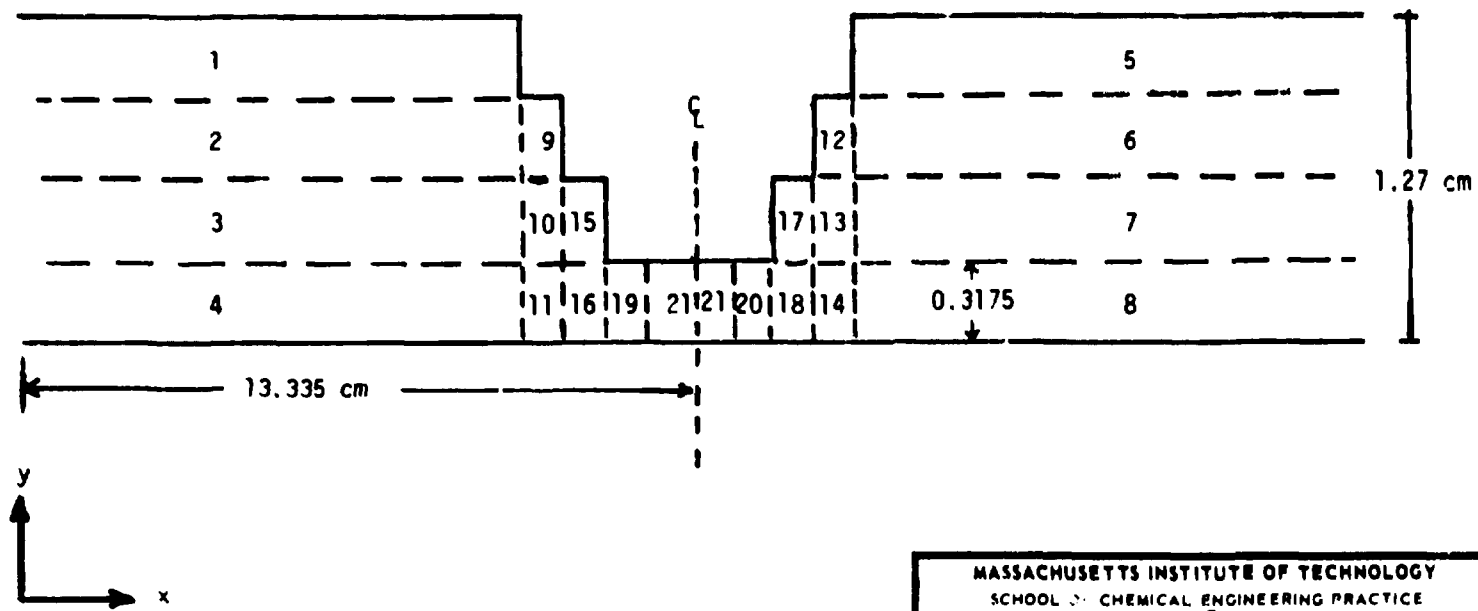

MASSACHUSETTS INSTITUTE OF TECHNOLOGY
SCHOOL OF CHEMICAL ENGINEERING PRACTICE
AT
OAK RIDGE NATIONAL LABORATORY

ASSIGNMENT OF REGIONS BEFORE FIRST PASS

DATE	DRAWN BY	FILE NO.	FIG.
12-19-76	JAP	CEPS-X-245	4

conduction from the hot filler directly under the arc. This assumption is justified since the filler rod is in contact with the weld pool in actual welding operations.

For the computer simulation heat enters the region directly below the arc at a constant heat flux. The arc cross-section is assumed to be square, with a width of 0.3704 cm. (The arc width was selected to assure symmetric heat input into the filler metal as described in Appendix 8.1.1.) The movement of the weld head is simulated by moving the heat flux in finite steps along the groove; the intensity of the heat flux used was the same as that encountered in actual welding operations. For a TIG welding efficiency of 0.40 (17), the actual rate of heat into the weldment can be calculated from:

$$Q_{gen} = (0.24\ cal/J)(I)(V)(EFF) \qquad (1)$$

where Q_{gen} is the heat generated, I is the amperage, V is the voltage, and EFF is the efficiency of energy transfer to the work piece. Then the heat flux through the region surface directly under the simulated arc can be calculated:

$$Q_{arc} = \frac{Q_{gen}}{A} \qquad (2)$$

where Q_{arc} is the heat flux and A is the cross-sectional area under the arc.

No quantitative descriptions of the mixing action could be found. However, based on data for lead (1) and the assumptions made for stainless steel in Westby's model (17), the effective conductivity of the molten metal under the arc was judged to be seven to eight times greater than that for stagnant molten metal at the same temperature. The computer model utilizes this high effective conductivity to simulate the mixing action in the turbulent zone. Heat is then assumed to be conducted (rather than convected) from this turbulent zone to the laminar zone where an effective conductivity approaching the conductivity of stagnant molten metal was assumed. Energy is thus transported through the entire HAZ by conduction. Heat is lost from the surface of the laminar and solid zones by natural convection and radiation. The surface of the turbulent zone is modeled so that radiation and convection does not occur since the heat flux into this surface is a net heat flux which already considers these effects.

3.2.3 Properties

Tabular functions were entered into the program to describe the temperature-dependent properties: thermal conductivity, specific heat, and the coefficients for horizontal and vertical natural convection and radiation.

Density was assumed to be constant (6). For AISI304 stainless steel, data for the thermal conductivity from 0 to 1200°C and specific heat from 50 to 1300°C were found in BISRA (3). The data for these two properties were extrapolated to the melting temperature since no data could be found in the literature for molten steels. Hence, the specific heat was assumed constant at 0.17 cal/gm-°C above 1450°C. The thermal conductivity at 1450°C for molten metal was taken as 0.25 cal/cm-°C-sec as suggested by Westby (17). This value reflects the slow convection currents expected to be found in the laminar zone. The temperature of the turbulent zone was expected to be a few degrees above the melting temperature (6). To simulate the strong convection currents found in this zone directly under the welding arc, an effective conductivity of 0.60 cal/cm-°C-sec was used for temperatures greater than 1460°C.

The equation in HEATING5 (16) for the overall surface heat transfer coefficient, is

$$h = h_f + h_r(T_S^2 + T_A^2)(T_S + T_A) + h_n(T_S - T_A)^{Ne} \qquad (3)$$

Forced convection would only occur on the edges of the wedge adjacent to the arc where the argon shield gas would flow up out of the weld. An order of magnitude analysis (Appendix 8.2.4) showed this term could be neglected. The radiation coefficient is the product of the Stephan-Boltzman constant and the temperature dependent emissivity of steel. The two coefficients for natural convection are predicted from an empirical correlation (13).

$$Nu = \frac{h_n L}{k} = a(GrPr)^{Ne} \qquad (4)$$

where a = 0.54 and Ne = 0.3333 for horizontal surfaces (hot side up), a = 0.27 and Ne = 0.3333 for horizontal surfaces (hot side facing down), and a = 0.41 and Ne_4 = 0.25 for vertical surfaces. These constants only hold for $10^4 < (Gr)(Pr) < 10^9$ and all terms are evaluated at

$$T_{film} = \frac{T_S + T_A}{2}$$

Stainless steel is a composite material; hence, it has a melting range of 1430 - 1470°C rather than a melting point. However, the required input for phase transitions for HEATING5 is a melting point and a heat of fusion. The melting point used in HEATING5 was 1450°C. The corresponding heat of fusion for 304 stainless steel is 65 cal/gm.

3.2.4 Mathematical Formulation

The Poisson equation which describes the isotropic, three-dimensional transient heat flow in the weldment is:

$$\rho C_p \frac{\partial T}{\partial t} = \frac{\partial}{\partial x}(k \frac{\partial T}{\partial x}) + \frac{\partial}{\partial y}(k \frac{\partial T}{\partial y}) + \frac{\partial}{\partial z}(k \frac{\partial T}{\partial z}) \quad (5)$$

Numerical solution of this partial differential equation by a forward finite difference technique requires dividing the slab into nodes and applying an energy balance around each node. The finite difference equation for node i is given by (16)

$$T_i^{n+1} = T_i^n + \frac{\Delta t}{C_i}\left[\sum_{m=1}^{M_i} K_{\alpha_m}(T_{\alpha_m}^n - T_i^n)\right] \quad (6)$$

Equation (6) predicts the temperature at each node at each successive time increment from the node temperatures and material properties at the preceding time increment. This procedure is known as the classical explicit method (CEP). The solution is stable if the time step satisfies the following stability criterion (5):

$$\Delta t \leq \left[\frac{C_i}{\sum_{m=1}^{M_i} K_{\alpha_m}}\right] \text{ minimum for all nodes} \quad (7)$$

It is only necessary to weld far enough along the groove to establish a quasi-steady state condition. This can save considerable computer time since the isotherms for the remainder of the weld length extending beyond that length necessary to achieve the quasi-steady state condition will be identical until the arc nears the other end of the slab.

4. RESULTS AND DISCUSSION

4.1 Results

By enlarging the region over which the heat flux acted to a square of 0.3704 cm on each side, it was possible to attain a symmetric heat input into the filler metal under the arc. As discussed in Appendix 8.1.2, increasing the length and width of the arc ensures that the arc completely covers the fine lattice lines which are in the region under the arc.

The subroutine which determines the position of the arc (described in Appendix 8.1.2) successfully moved the arc down the filler metal. Heat input from the arc melted the weld surface first and then nodes below the

surface, as was expected. Tables 1 and 2 show the change with time of the ratio of the mass of melted metal to mass of total metal contained in the node volume (melting ratio) for the nodes directly under the center of the arc. Some unexpected fluctuations in the melting ratios due to the inaccuracies of the solution can be seen in both tables.

For the CEP, the initial stable time step was determined to be 0.0168 sec. After thirteen time increments, the stable time step had decreased to 0.00732 sec because the temperature-dependent properties and surface heat losses had increased as the temperature of the slab increased. When the calculated stable time increment becomes an order of magnitude less than the stable time increment, the case will be deleted. To use the CEP, a stable time step of $\Delta t \leq 0.001$ is necessary. A time step of this size would require unreasonable amounts of computer time; hence, an alternative to the CEP was sought. Levy's modification to the CEP appeared to offer some relief. In Levy's modification the stable time increment can be multiplied by a user-specified factor and then a Z-factor is calculated by the computer to assure stability of the solution. This method is described in fuller detail in the HEATING5 manual (16) and in Appendix 8.1.1. Although this solution is always stable, the appropriate Levy multiplication factor must be selected to attain suitable accuracy. A Levy factor of five (Levy time step of 0.037 sec) yielded a solution which was reasonably accurate for short times; Fig. 5 shows the isotherms predicted after simulation of 1.5 sec of welding. At longer times the solution becomes less accurate as illustrated in Fig. 6. This shows the growing oscillations in the predicted temperature history for a node located on the top surface of the filler material under the arc. The inaccuracies introduced by selection of different Levy's multiplication factors are dramatized in Tables 3 and 4, generated with Levy's time steps of 0.147 and 0.037 sec, respectively. The solution becomes inaccurate at very short times after implementation of the Levy time step and blows up as the simulated welding time approaches 7 sec. The caution issued in the HEATING5 manual that, "of course, one must experiment with the size of the time step to obtain an acceptable solution" is hence well advised. While no acceptable Levy time step was determined in this project, further attempts to determine an acceptable time step appear necessary if reasonable CPU times are ever to be attained.

4.2 Discussion of Results

The best case attained during computer simulation was that generated with the Levy time of 0.037 sec. In this case, a marginally stable simulation of 2.62 sec of welding (0.55 cm down the groove) was attained in 80 min of CPU time. Paley and Hibbert (11) suggest that a quasi-stationary state should be achieved in about 7 sec of welding time. Hence, even if the Levy time step of 0.037 sec was acceptable, it would still require 214 min of CPU time to simulate 7 sec of welding. Perhaps more propitious spacing of the fine lattice lines and elimination of any unnecessary nodes could reduce the necessary CPU time.

Table 1. Melting Ratios for the Plane z = 0.3175*

Levy's Time Step = 0.03744 sec

Center of Slab

7 Time Steps, Time = 0.1581 sec

Distance → x	13.21	13.29	13.38	13.46
0.0	0.0	0.0	0.0	0.0
0.11	0.0	0.0	0.0	0.0
0.21	0.0	0.0	0.0	0.0
y ↓ 0.32	0.0	0.21	0.21	0.0
0.64				
0.95				
1.27				

9 Time Steps, Time = 0.2025 sec

Distance → x	13.21	13.29	13.38	13.46
0.0	0.0	0.0	0.0	0.0
0.11	0.0	0.0	0.0	0.0
0.21	0.0	0.0	0.0	0.0
y ↓ 0.32	0.0	0.77	0.77	0.0
0.64				
0.95				
1.27				

16 Time Steps, Time = 0.2995 sec

Distance → x	13.12	13.21	13.29	13.38	13.46	13.55
0.0	0.0	0.0	0.0	0.0	0.0	0.0
0.11	0.0	0.0	0.0	0.0	0.0	0.0
0.21	0.0	0.0	0.0	0.0	0.0	0.0
y ↓ 0.32	0.0	1.00	1.00	1.00	1.00	0.0
0.64	0.0					0.0
0.95						
1.27						

23 Time Steps, Time = 0.5615 sec

Distance → x	13.12	13.21	13.29	13.38	13.46	13.55
0.0	0.0	0.0	0.0	0.0	0.0	0.0
0.11	0.0	0.0	0.0	0.0	0.0	0.0
y ↓ 0.21	0.0	0.0	0.0	0.0	0.0	0.0
0.32	0.0	0.71	1.00	1.00	0.71	0.0
0.64	0.0					0.0
0.95						
1.27						

*Top of metal surface is at y = 0.32 (see Fig. 4).

Table 2. Melting Ratios for the Plane z = 0.6350

Levy's Time Step = 0.03744 sec

Center of Slab ↓

52 Time Steps, Time = 1.6476 sec

Distance → x	13.12	13.21	13.29	13.38	13.46	13.55
0.0	0.0	0.0	0.0	0.0	0.0	0.0
y ↓ 0.11	0.0	0.0	0.0	0.0	0.0	0.0
0.21	0.0	1.00	0.55	0.55	1.00	0.0
0.32	1.00	0.0	1.00	1.00	0.0	1.00
0.64	0.0					0.0
0.95						
1.27						

56 Time Steps, Time = 1.7974 sec

Distance → x	13.07	13.12	13.21	13.29	13.38	13.46	13.55	13.60
0.0	0.0	0.0	0.0	1.0	0.0	0.0	0.0	0.0
y ↓ 0.11	0.0	0.0	1.00	0.0	0.0	1.00	0.0	0.0
0.21	1.00	0.96	0.73	1.00	1.00	0.73	0.96	1.00
0.32	0.0	1.00	1.00	1.00	1.00	1.00	1.00	0.0
0.64	0.0	0.0					0.0	0.0
0.95	0.0							0.0
1.27								

61 Time Steps, Time = 1.9846 sec

Distance → x	13.07	13.12	13.21	13.29	13.38	13.46	13.55
0.0	0.0	0.0	0.41	1.00	1.00	0.38	0.0
y ↓ 0.11	0.0	1.00	0.64	1.00	1.00	0.65	0.99
0.21	0.0	1.00	1.00	1.00	1.00	1.00	1.00
0.32	1.00	0.85	1.00	1.00	1.00	1.00	0.85
0.64	0.0	0.0				0.0	0.0
0.95	0.0						0.0
1.27							

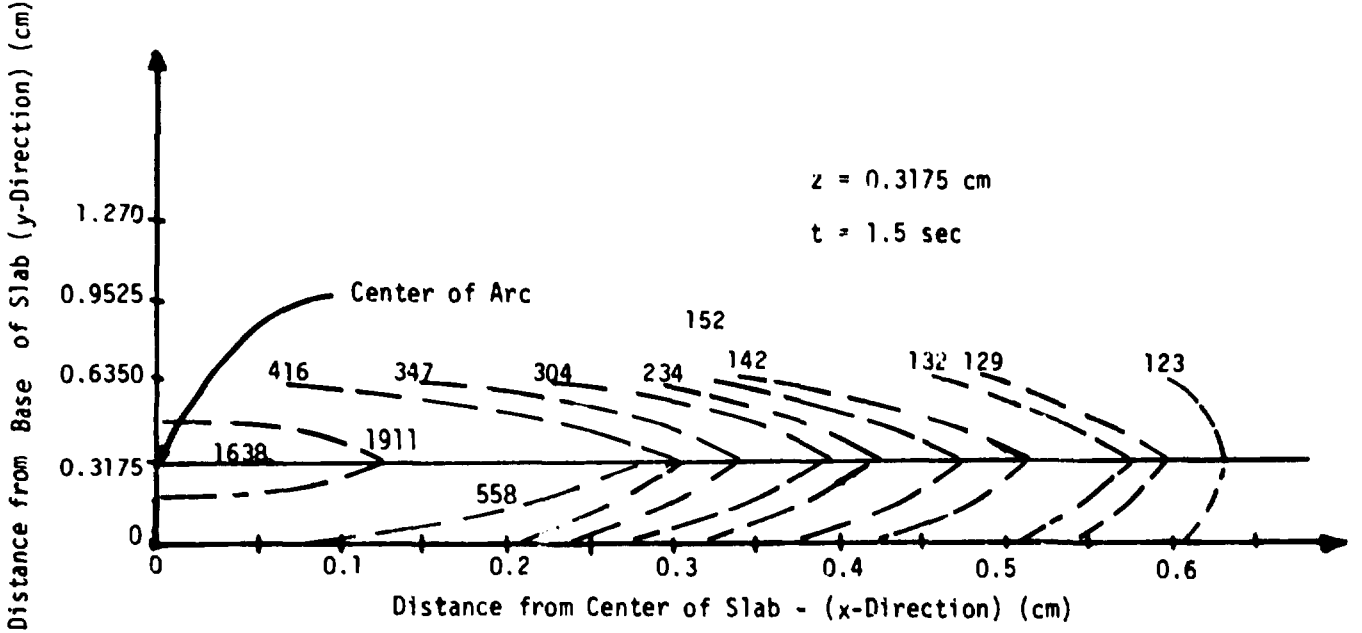

MASSACHUSETTS INSTITUTE OF TECHNOLOGY
SCHOOL OF CHEMICAL ENGINEERING PRACTICE
AT
OAK RIDGE NATIONAL LABORATORY

ISOTHERMS IN X-Y PLANE
PREDICTED BY HEATING5

DATE	DRAWN BY	FILE NO.	FIG.
12-19-76	PKW	CEPS-X-245	5

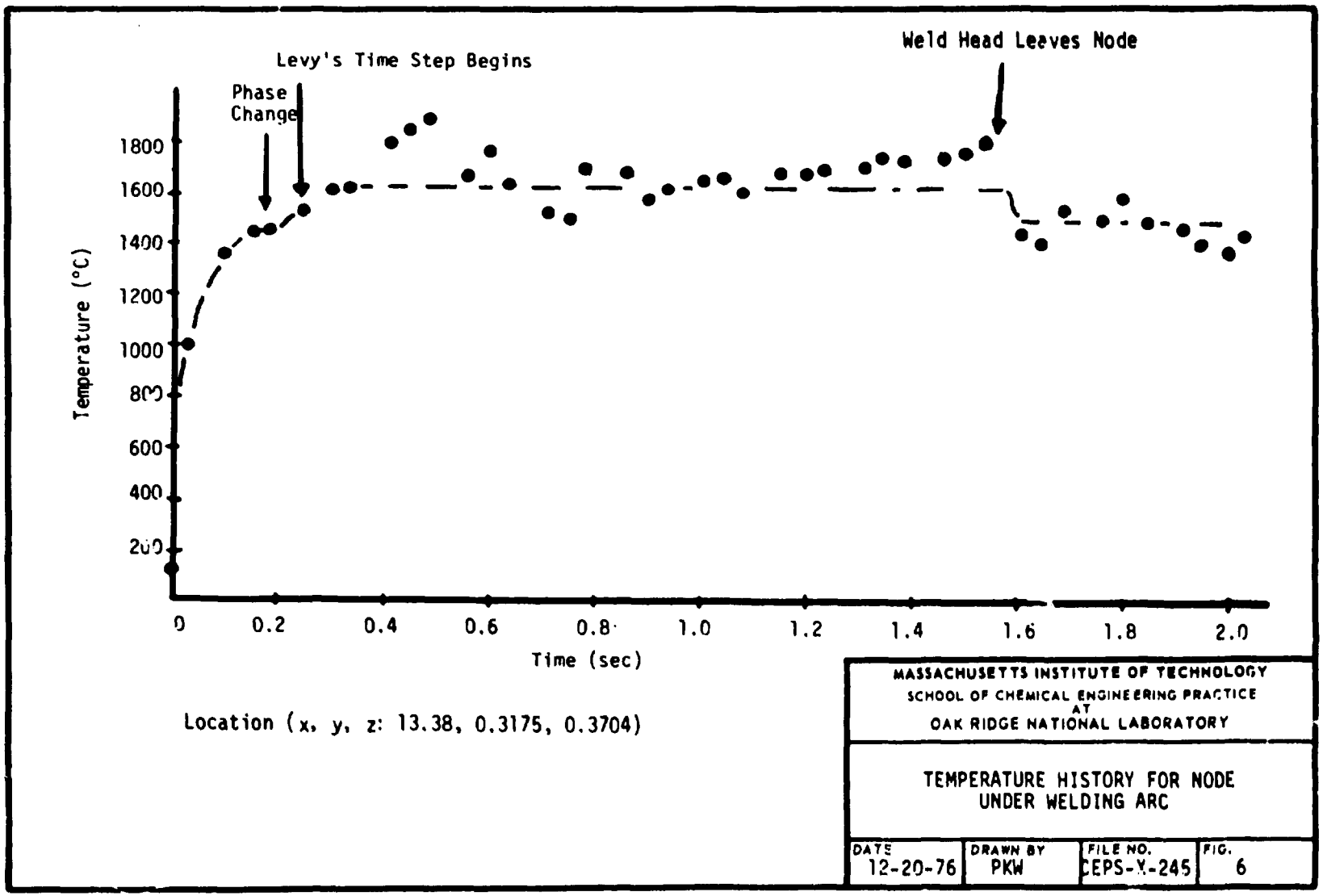
Levy's Time Step Begins
Phase Change
Weld Head Leaves Node
Temperature (°C)
1800
1600
1400
1200
1000
800
600
400
200
0
0.2
0.4
0.6
0.8
1.0
1.2
1.4
1.6
1.8
2.0
Time (sec)
Location (x, y, z: 13.38, 0.3175, 0.3704)
MASSACHUSETTS INSTITUTE OF TECHNOLOGY
SCHOOL OF CHEMICAL ENGINEERING PRACTICE
AT
OAK RIDGE NATIONAL LABORATORY
TEMPERATURE HISTORY FOR NODE
UNDER WELDING ARC
DATE 12-20-76
DRAWN BY PKW
FILE NO. CEPS-Y-245
FIG. 6

Table 3. TRANSIENT TEMPERATURE DISTRIBUTION AFTER 41 TIME STEPS. TIME = 1.988450 00
FOR THE PLANE Z = 6.350000D-01, Levy Time Step = 0.127 sec

DISTANCE → x / y ↓	0.0	4.23	8.47	12.70	12.75	12.81	12.86	12.91	12.96	13.02	13.07	13.12	13.21
0.0	120188	*****	*****	*****	*****	*****	*****	*****	*****	*****	*****	*****	*****
0.11	120195	120.96	120.96	126.22	160.20	191.44	224.62	262.12	305.60	352.39	416.87	603.63	739.45
0.21	121100	121.01	121.01	126.22	153.90	181.08	210.22	251.12	290.89	357.21	754.46	1280.11	1468.14
0.32	121103	121.04	121.05	125.78	148.42	168.91	195.68	218.10	249.50	454468	*****	*****	*****
0.64	121106	121.07	121.07	122.44	128.10	133.78	138***	*****	*****	*****	0.0	0.0	0.0
0.95	121100	121.01	121.01	121***	*****	*****	*****	0.0	0.0	0.0	0.0	0.0	0.0
1.27	120178	*****	*****	*****	0.0	0.0	0.0	0.0	0.0	0.0	0.0	0.0	0.0

DISTANCE → x / y ↓	13.29	13.38	13.46	13.55	13.60	13.65	13.71	13.76	13.81	13.86	13.92	13.97	18.20
0.0	*****	*****	*****	*****	*****	*****	*****	*****	*****	*****	*****	*****	*****
0.11	844.35	844.36	739.43	603.53	416.87	352.45	305.62	262.12	224.59	191.42	160.20	126.23	120.96
0.21	1450.00	1450.00	1468.12	1279.78	754.45	357.26	290.89	251.10	210.19	181.06	153.88	126.22	121.01
0.32	*****	*****	*****	*****	*****	464.88	249.45	218.07	195.93	168.89	148.41	125.78	121.05
0.64	0.0	0.0	0.0	0.0	0.0	187***	*****	*****	133.77	128.05	122.44	121.07	
0.95	0.0	0.0	0.0	0.0	0.0	0.0	0.0	0.0	123***	*****	*****	121.01	
1.27	0.0	0.0	0.0	0.0	0.0	0.0	0.0	0.0	0.0	0.0	0.0	*****	*****

DISTANCE → x / y ↓	22.44	26.67
0.0	*****	*****
0.11	120.96	120195
0.21	121.01	121100
0.32	121.04	121103
0.64	121.07	121106
0.95	121.01	121100
1.27	*****	*****

Table 4. TRANSIENT TEMPERATURE DISTRIBUTION AFTER 61 TIME STEPS, TIME = 1.984650 00
FOR THE PLANE Z = 6.350000-01, Levy Time Step = 0.037447 sec

DISTANCE ↓ y / x →	0.0	4.23	8.47	12.70	12.75	12.81	12.86	12.91	12.96	13.02	13.07	13.12	13.21
0.0	120188	[illegible]	[illegible]	[illegible]	[illegible]	[illegible]	[illegible]	[illegible]	[illegible]	[illegible]	[illegible]	[illegible]	[illegible]
0.11	120195	120.96	120.97	129.75	180.94	257.25	346.93	477.53	600.30	826.78	1142.37	1450.00	1450.00
0.21	121100	121.01	121.01	129.45	194.92	270.58	376.73	479.75	693.23	1044.63	1160.30	1956.20	1457.87
0.32	121103	121.04	121.05	128.60	179.04	239.05	331.94	466.72	596.81	776[illegible]	[illegible]	[illegible]	[illegible]
0.64	121106	121.07	121.07	123.37	133.02	144.04	155[illegible]	[illegible]	[illegible]	[illegible]	0.0	0.0	0.0
0.95	121100	121.01	121.01	121[illegible]	[illegible]	[illegible]	[illegible]	0.0	0.0	0.0	0.0	0.0	0.0
1.27	120178	[illegible]	[illegible]	[illegible]	0.0	0.0	0.0	0.0	0.0	0.0	0.0	0.0	0.0

DISTANCE ↓ y / x →	13.29	13.38	13.46	13.55	13.60	13.65	13.71	13.76	13.81	13.86	13.92	13.97	18.20
0.0	[illegible]	[illegible]	[illegible]	[illegible]	[illegible]	[illegible]	[illegible]	[illegible]	[illegible]	[illegible]	[illegible]	[illegible]	[illegible]
0.11	1466.97	1465.77	1450.00	1450.00	1185.67	827.08	600.45	477.60	346.87	257.25	180.94	129.75	120.97
0.21	1714.45	1714.50	1461.82	1956.60	1165.17	1045.04	693.30	479.78	376.71	270.58	194.64	129.45	121.01
0.32	[illegible]	[illegible]	[illegible]	[illegible]	[illegible]	[illegible]	596.82	465.69	331.90	239.04	179.08	128.61	121.05
0.64	0.0	0.0	0.0	0.0	0.0	216[illegible]	[illegible]	[illegible]	[illegible]	144.03	133.01	123.37	121.07
0.95	0.0	0.0	0.0	0.0	0.0	0.0	0.0	0.0	124[illegible]	[illegible]	[illegible]	[illegible]	121.01
1.27	[illegible]	[illegible]	[illegible]	[illegible]	[illegible]	[illegible]	[illegible]	[illegible]	[illegible]	[illegible]	[illegible]	[illegible]	[illegible]

The second problem encountered in this simulation is that the temperature of the molten metal does not peak at a few degrees above the melting temperature as would be expected. The almost order-of-magnitude difference between the thermal conductivity of the solid metal and that of the molten metal appears to force the solid metal to behave like an adiabatic wall, hence heat accumulates in the turbulent pool and temperatures at the solid/molten interface are higher than those at the center of the pool. (This effect can be observed in Fig. 6.) Two possible explanations for the occurrence of this effect in the computer simulation and not in experimental results can be proposed. Kreith (14) suggests that the thermal conductivity of some alloys decreases sharply as the metal melts and then increases steeply to the conductivity of the solid at T_{melt} after melting. This would decrease the sharp difference in thermal conductivities at the molten/solid interface and allow heat to flow quickly out of the molten region as expected. A second contributing effect is that the distribution of the intensity of the arc is actually bell-shaped so that the region at the outer radius under the arc receives perhaps 5% of the total heat flux received at the center of the region under the arc (11, 12). Inputting a bell-shaped heat flux distribution might also elevate the problem of lower temperatures at the center of the molten pool than at the edges.

A second problem arises in the temperature profiles under the arc; the surfaces below the top surface of the weldment appear to heat faster and remain molten longer than the top surface. This effect could be due to inaccuracies induced by the too-large time step or once again could be a function of the large difference between the thermal conductivity of the molten metal and the solid metal. This effect is seen in Table 3.

For small time steps (or short times) HEATING5 predicts reasonable temperature profiles. Temperatures drop slightly in regions which are too far from the welding heat to receive heat. (Radiation and convection losses from a slab at 121°C.) Regions under the arc melt and resolidify after the arc passes. Reasonable temperature profiles are attained for short times.

5. CONCLUSIONS

HEATING5 can be used to predict the temperature history of a multipass filled weldment. It provides a general solution which can handle a variety of situations, including various weld angles and shapes, filler metal which differs from the base metal composition, temperature-dependent properties, and radiation and convection boundary conditions. However, substantial work is still required to refine this program and substantial convergence of the predicted solutions.

6. RECOMMENDATIONS

This project has indicated that HEATING5 can be used to solve the desired heat transfer problem. However, the computer program as it is presented is not capable of predicting an accurate solution in a reasonable amount of CPU time. Refinements which must be considered include:

1. Adjust the Levy's factor time increment and/or multiplication factor and the spacing of fine lattice lines to obtain an acceptably stable solution in the minimum necessary time.

2. Experimentally determine k_{eff} in the molten metal, both for the turbulent and laminar regions, or

3. Empirically control the molten pool size by addition of a time/position dependent k_{eff} with a more gradual increase in k_{eff} from T_{melt} to T_{turb}, or

4. Revert to an empirical approach for determining the turbulent and laminar pool boundaries and specify the heat flux from the turbulent pool in a manner similar to those outlined in the works of Pavelic *et al.* (12) and Kleinschmidt *et al.* (6).

5. Add heat from the arc with a bell-shaped intensity as described in the works of Pavelic *et al.* (12) and Paley and Hibbert (11).

6. Perform case studies to check for sensitivity of temperature profiles to parameters of known effect such as arc speed and intensity, C_p, k_{eff}, and k_{solid}.

7. Implement the implicit method of solution when it becomes available on HEATING5.

In addition, it might be beneficial to investigate further refinements once the basic computer simulation technique has been completed. Included in these refinements are the following:

1. Implement necessary subroutines to simulate cases where base metal and filler metal are of different composition.

2. Develop an algorithm to implement multiple passes without preheating the slab to 121°C before each pass. This requires relating the positions of nodes from previous passes in a logical manner and initializing the slab at the appropriate temperature profile.

3. Review the work conducted by Muraki *et al* (10) which combines prediction of temperature profiles and residual stresses and strains for modifications applicable to HEATING5.

7. ACKNOWLEDGMENTS

We would like to thank G.W. Goodwin, J.F. King, and D. Edmonds for their assistance. Special thanks go to Jay Dweck for his magnanimous contributions: moral support, helpful suggestions, and much time.

8. APPENDIX

8.1 HEATING5

8.1.1 First Implementation

Transient conduction problems may be solved by one of several methods. The classical explicit procedure involves the first forward time difference with respect to time. The method gives stabile solutions only when the time step used is less than a specified stability criterion. A modification of the classical explicit procedure that is stabile for any time step may be employed. Implicit solutions are computed by using the Crank-Nicholson or classical implicit procedure, or a linear combination of both. The finite difference equations used in the implicit method are solved by point successive over-relaxation iteration. In steady-state simulations, the finite difference equations are solved by the point successive over-relaxation iteration and a modification of the "Aitken δ^2 Extrapolation Process" (16).

HEATING5 requires that the problem be defined in a certain way. The configuration of the problem is approximated by dividing it into regions. The general shape of the problem, its material composition, and any irregular shapes determine the placement, size, and number of regions used. A maximum of 100 regions is allowed. The regions are formed by the intersection of lattice lines that run the length of the problem. A set of lattice lines is parallel to the axis in the same direction and perpendicular to all other axes. Subdivision of the regions by fine lattice lines is done if the problem requires. The resulting mesh of lattice lines is used in the solution of the finite difference equations.

The parameters needed to describe the material(s) in the regions are entered into HEATING5 as constants, analytical functions, or tabular functions. Appropriate boundary conditions are entered in the same fashion. If the tabular or analytic function options are unable to adequately describe a parameter, a user-supplied subroutine is employed. The simulation must be specified as transient, steady-state, or as an alternating series of steady-state and transient simulations. Finally, the type of solution (explicit or implicit) must be specified.

All input data and any user-supplied subroutines are listed by HEATING5. A map of the nodes assigned to the problem and a map of the initial temperature distribution are printed. For transient simulations, maps of temperature distribution vs time are printed. Only the final temperature distribution is printed for steady-state problems. For problems involving phase changes, maps of melting ratios are printed after each temperature distribution (the melting ratio is defined as the ratio of heat which has been absorbed after the transition temperature has been reached to the total heat needed to complete the phase change for a material in node i). The node, temperature distribution, and melting ratio maps are x-y plots

for each incremental z position. Thus, the output consists of a series of two-dimensional maps.

Three subroutines are used to describe the phenomenon on the upper horizontal surface of the weld rod. As the weld head moves down the length of the weld rod in finite steps equal to the time step of the problem times the weld head velocity, a specified heat is fluxed in through the surface of this rod directly below the weld head. For the rest of the surface of the rod, the specified heat flux in is zero, and the surface radiates and convects heat.

The subroutine to specify the inward heat flux is listed in Table 6. The position and width of the weld beam in the X-axis are constant with time.

Table 6. User-Supplied Subroutine 1 for Specified Boundary Flux Directly Under Weld Head

```
      SUBROUTINE BNFLUX(RVALUE,R,TH,Z,TIM, TSN, VALUE,NUMBER,N)
       REAL*8 RVALUE,R,TH,Z,TIM,TSN,VALUE
      COMMON /INOUT/  IN ,IO
     ************************************************************
     *                  *USER SUPPLIED SUBROUTINE*              *
     *                  **************************              *
     *THIS SUBROUTINE WILL ASSIGN THE PRESCRIBED HEAT FLUX TO THE*
     *INCREMENTAL AREA DIRECTLY UNDER THE WELD BEAM.  THE HEAT   *
     *FLUX TO ALL OTHER INCREMENTAL AREAS WILL BE ZERO.          *
     ************************************************************
      VEL=.21
     *LOWER Z-BOUNDARY OF THE WELD HEAD
      ZBOUN1=VEL*TIM
     *UPPER Z-BOUNDARY OF THE WELD HEAD
      ZBOUN2=VEL*TIM+0.3704
     *LOWER X-BOUNDARY OF THE WELD HEAD
      RBOUN1=13.1499
     *UPPER X-BOUNDARY OF THE WELD HEAD
      RBOUN2=13.5203
      IF(Z.LE.ZBOUN2.AND.Z.GE.ZBOUN1) GO TO 10
      GO TO 20
10    CONTINUE
      IF(R.LE.RBOUN2.AND.R.GE.RBOUN1) GO TO 30
20    RVALUE=0.
      RETURN
30    RVALUE=1030.
      RETURN
      END
```

The position of the weld beam along the z-axis is time-dependent. The subroutine calculates the position of the weld arc and two logical arguments to determine the area through which the heat is fluxed in. Where the arguments are not satisfied, the heat flux is zero.

Heat enters and leaves only through nodes, not through surfaces. Boundary nodes are divided between the regions that they separate. If the welding arc is positioned to sit exactly on top of a node, then any small fluctuation in node position due to a computer round-off error will cause the heat flux in to be unsymmetrical. Therefore the width and depth of the weld arc are specified so that the weld beam completely covers the fine lattice lines that are in the region of heat input. This assures that the heat input will be symmetrical.

The subroutines used to calculate the radiation and natural convection from the weld rod surface not directly under the weld head are listed in Tables 7 and 8. These subroutines determine the position and dimensions of the weld beam exactly as described before. By using logical arguments that are the converse of the arguments used in subroutine BNFLUX, the subroutines determine whether radiation and convection occur. If the arguments are satisfied, the subroutine RADITN calls analytical function 3 to calculate radiation and subroutine NATCON calls analytical function 4 to calculate the natural convection. The exponent used in natural convection is constant with temperature and is listed in the data deck on the card for the boundary of the weld rod. If the arguments are not satisfied, radiation and convection are zero.

Table 7. User-Supplied Subroutine 2 for Specifying Radiation from Weld Rod Not Directly Under Weld Head

```
      SUBROUTINE RADITN(RVALUE,R,TH,Z,TIM,TSN,VALUE,NUMBER,N)
      REAL*8 RVALUE,R,TH,Z,TIM,TSN,VALUE
      COMMON /INOUT/  IN ,IO
     ************************************************************
     *                    *USER SUPPLIED SUBROUTINE*            *
     *                    ***************************           *
     *THIS SUBROUTINE WILL ASSIGN THE RADIATION COEFFICIENT AS A  *
     *FUNTION OF TEMPERATURE FOR THE SURFACE AREA OF THE WELDING  *
     *ROD THAT IS NOT DIRECTLY UNDER THE WELD HEAD.               *
     ************************************************************
      VEL=.21
     *LOWER Z-BOUNDARY OF THE WELD HEAD
      ZBOUN1=VEL*TIM
     *UPPER Z-BOUNDARY OF THE WELD HEAD
      ZBOUN2=VEL*TIM+.3704
     *LOWER X-BOUNDARY OF WELD HEAD
      RBOUN1=13.1499
     *UPPER X-BOUNDARY OF WELD HEAD
      RBOUN2=13.5203
      IF(Z.GT.ZBOUN2.OR.Z.LT.ZBOUN2) GO TO 10
      GO TO 20
10    CONTINUE
      IF(R.LE.RBOUN2.AND.R.GE.RBOUN1) GO TO 30
20    RVALUE=0.
      RETURN
30    CALL TABLE(-3,VALUE,TSN,RVALUE,N,NUMBER)
      RETURN
      END
```

Table 8. User-Supplied Subroutine 3 for Specifying Natural Convection from Weld Rod Surface Not Directly Under Weld Head

```
      SUBROUTINE NATCON(RVALUE,R,TH,Z,TIM,TSN,VALUE,NUMBER,N)
      REAL*8 RVALUE,R,TH,Z,TIM,TSN,VALUE
      COMMON /INOUT/  IN ,IO
*****************************************************************
*                        *USER SUPPLIED SUBROUTINE*
*                        ***************************
*THIS SUBROUTINE WILL ASSIGN THE NATURAL CONVECTION COEFFICIENT
*AS A FUNCTION OF TEMPERATURE FOR THE SURFACE AREA OF THE WELDING
*ROD NOT DIRECTLY UNDER THE WELDING HEAD.
*****************************************************************
      VEL=.21
*LOWER Z-BOUNDARY OF THE WELD HEAD
      ZBOUN1=VEL*TIM
*UPPER Z-BOUNDARY OF THE WELD HEAD
      ZBOUN2=VEL*TIM+.3704
*LOWER X-BOUNDARY OF WELD HEAD
      RBOUN1=13.1499
*UPPER X-BOUNDARY OF WELD HEAD
      RBOUN2=13.5203
      IF(Z.GT.ZBOUN2.OR.Z.LT.ZBOUN2) GO TO 10
      GO TO 20
10    CONTINUE
      IF(R.LE.RBOUN2.AND.R.GE.RBOUN1) GO TO 30
20    RVALUE=0.
      RETURN
30    CALL TABLE(-4,VALUE,TSN,RVALUE,N,NUMBER)
      RETURN
      END
```

8.1.2 Execution of Subsequent Weld Passes

Just as HEATING5 was used to obtain the temperature profile of the first pass of a multipass weld, it can be used to simulate the second through tenth passes of the weld head necessary to complete the weldment.

The minimum number of regions needed to approximate the weldment V-groove decreases with subsequent passes of the weld head. The boundary conditions used in describing the first pass are still valid. The user-supplied subroutines are still used. Only the upper and lower x-boundaries have to be adjusted to move the weld head over the region to be welded. Figures 7 through 15 contain a suggested scheme of placing the second through tenth filler rods.

To determine the peak temperature of each node and the amount of time that the node spends at a temperature greater than 730°C, a subroutine modification to HEATING5 will have to be undertaken. This routine must be able to determine at which time step the temperature of a node exceeded 730°C and at which time the temperature dropped below 730°C. The routine must also make provisions to record the peak temperature of the node during that simulation. This time and peak temperature data could be stored as a punched deck or on a tape or disk. A separate routine would then accumulate the time for each pass that each node spends above 730°C.

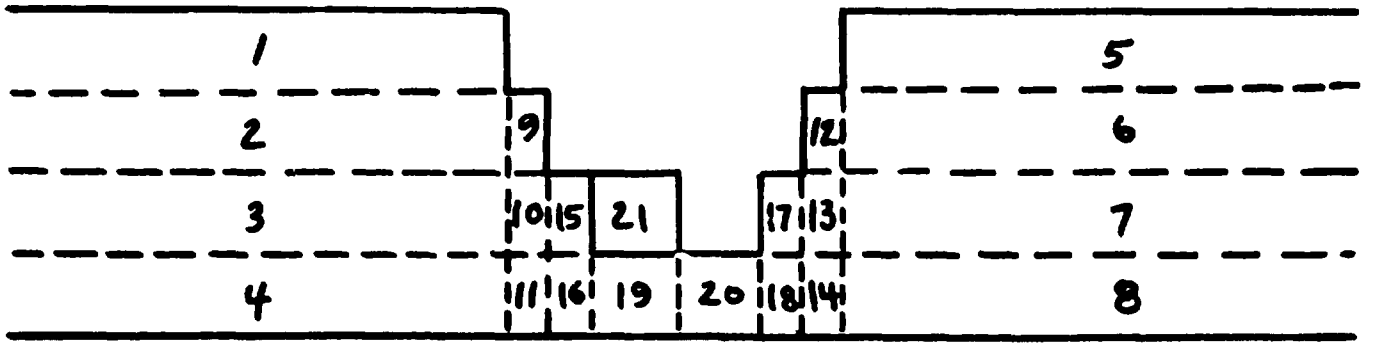

MASSACHUSETTS INSTITUTE OF TECHNOLOGY
SCHOOL OF CHEMICAL ENGINEERING PRACTICE
AT
OAK RIDGE NATIONAL LABORATORY

ASSIGNMENT OF REGIONS IN MULTI-PASS WELDMENT 2nd PASS

DATE	DRAWN BY	FILE NO.	FIG.
12/21/76	JAP	K-245	7

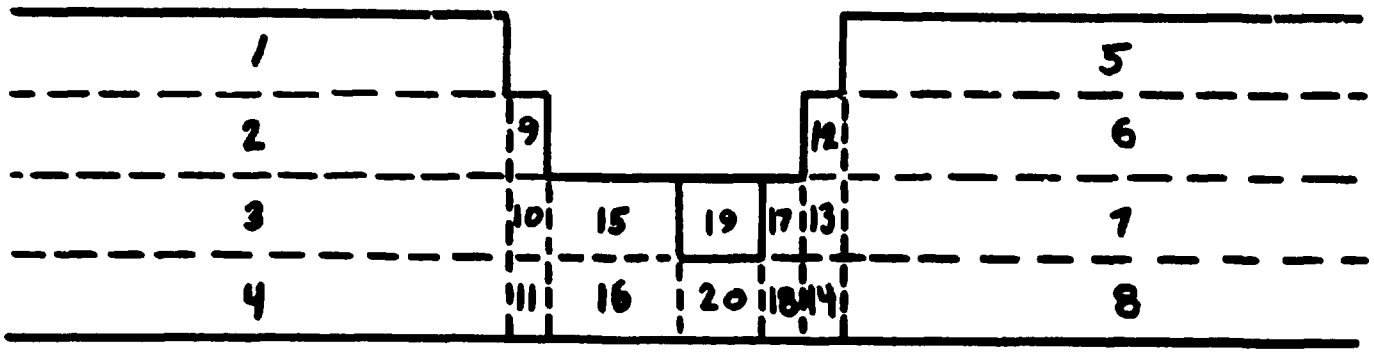

MASSACHUSETTS INSTITUTE OF TECHNOLOGY
SCHOOL OF CHEMICAL ENGINEERING PRACTICE
AT
OAK RIDGE NATIONAL LABORATORY

ASSIGNMENT OF REGIONS IN MULTI-PASS WELDMENT 3rd PASS

DATE	DRAWN BY	FILE NO.	FIG.
12/21/76	JAP	X-245	8

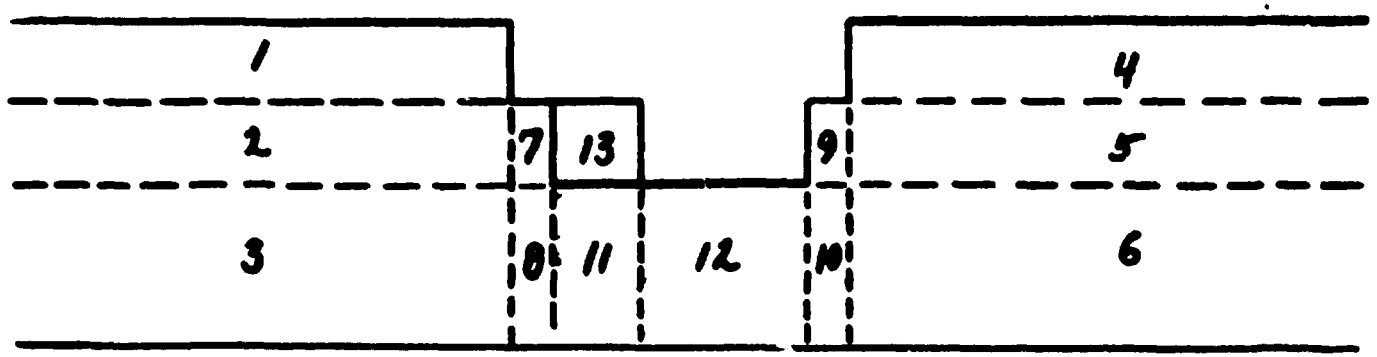

MASSACHUSETTS INSTITUTE OF TECHNOLOGY
SCHOOL OF CHEMICAL ENGINEERING PRACTICE
AT
OAK RIDGE NATIONAL LABORATORY

ASSIGNMENT OF REGIONS IN MULTI-PASS WELDMENT 4th PASS

DATE	DRAWN BY	FILE NO.	FIG.
12/21/76	JAP	X-245	9

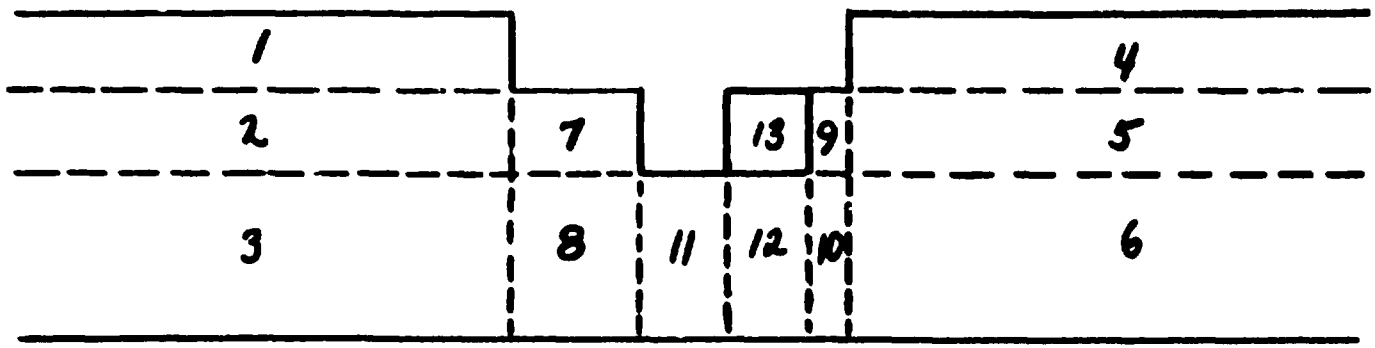

MASSACHUSETTS INSTITUTE OF TECHNOLOGY
SCHOOL OF CHEMICAL ENGINEERING PRACTICE
AT
OAK RIDGE NATIONAL LABORATORY

ASSIGNMENT OF REGIONS IN MULTI-PASS WELDMENT 5th PASS

DATE	DRAWN BY	FILE NO.	FIG.
12/21/76	JAP	X-245	10

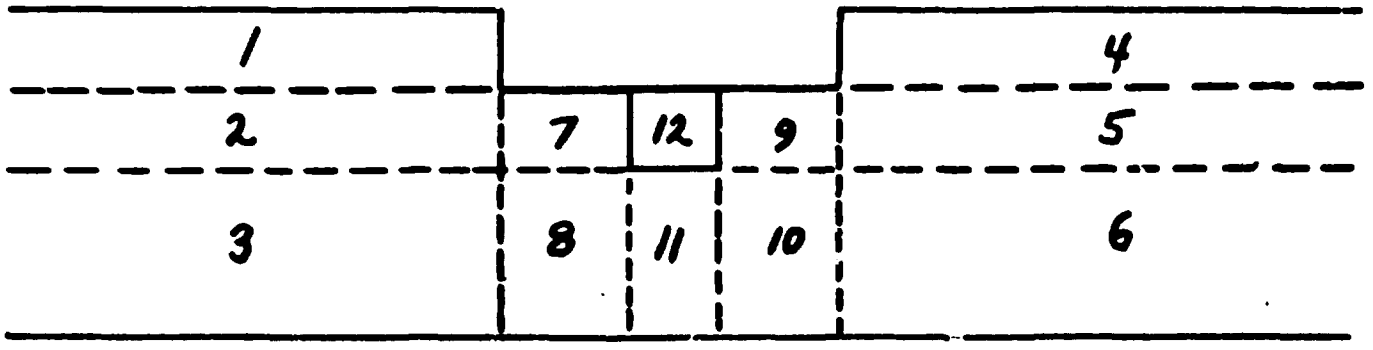

MASSACHUSETTS INSTITUTE OF TECHNOLOGY
SCHOOL OF CHEMICAL ENGINEERING PRACTICE
AT
OAK RIDGE NATIONAL LABORATORY

ASSIGNMENT OF REGIONS IN MULTI-PASS WELDMENT 6th PASS

DATE	DRAWN BY	FILE NO.	FIG.
12/21/76	JAP	X-245	11

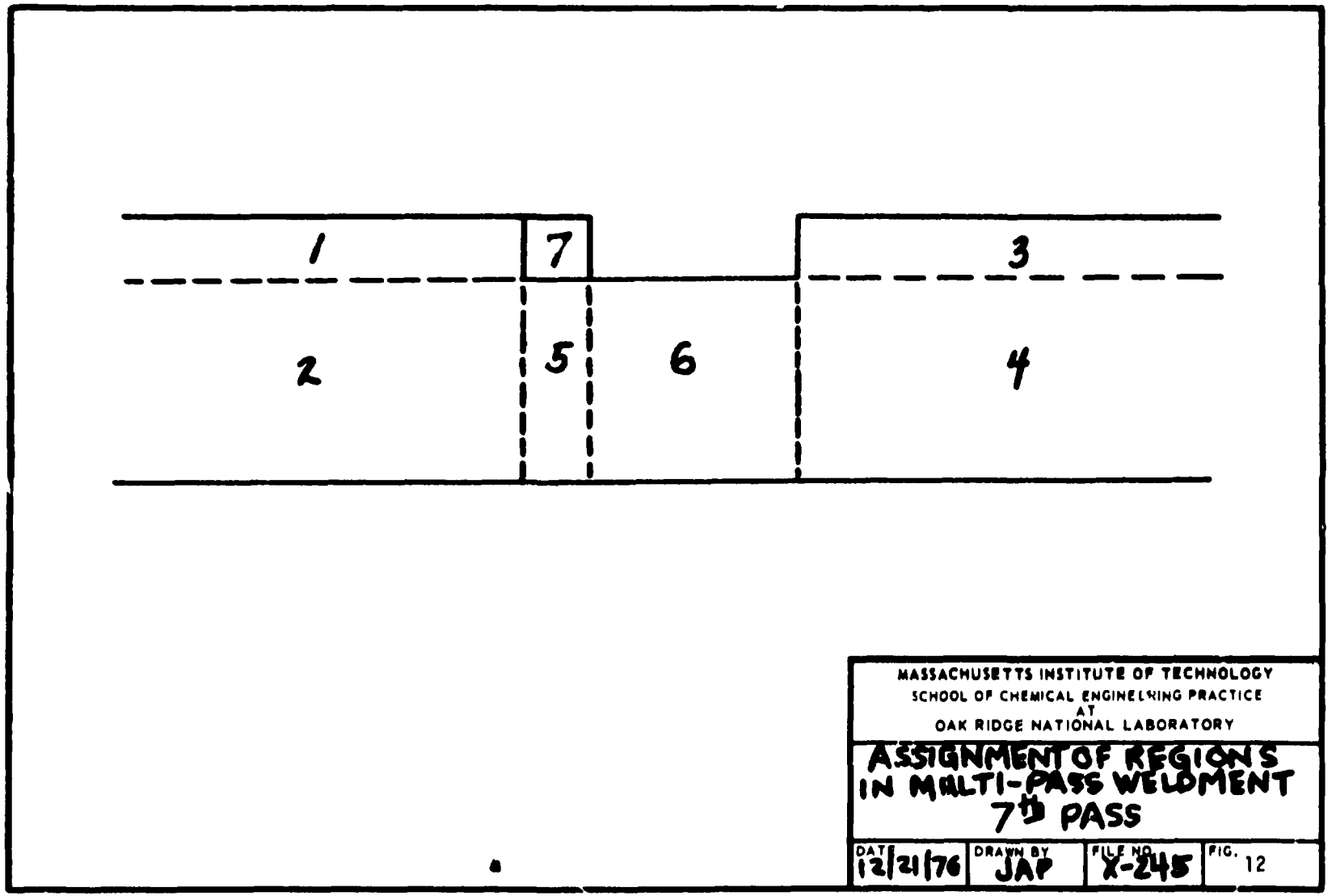

MASSACHUSETTS INSTITUTE OF TECHNOLOGY
SCHOOL OF CHEMICAL ENGINEERING PRACTICE
AT
OAK RIDGE NATIONAL LABORATORY

ASSIGNMENT OF REGIONS IN MULTI-PASS WELDMENT 7th PASS

DAT	DRAWN BY	FILE NO.	FIG.
12/21/76	JAP	X-245	12

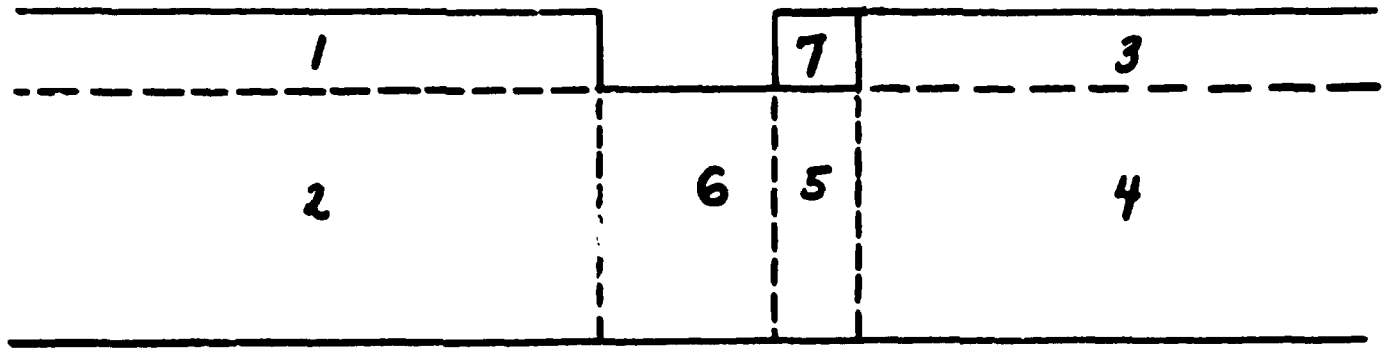

MASSACHUSETTS INSTITUTE OF TECHNOLOGY
SCHOOL OF CHEMICAL ENGINEERING PRACTICE
AT
OAK RIDGE NATIONAL LABORATORY

ASSIGNMENT OF REGIONS IN MULTI-PASS WELDMENT 8TH PASS

DATE	DRAWN BY	FILE NO.	FIG.
12/21/76	JAP	X-245	13

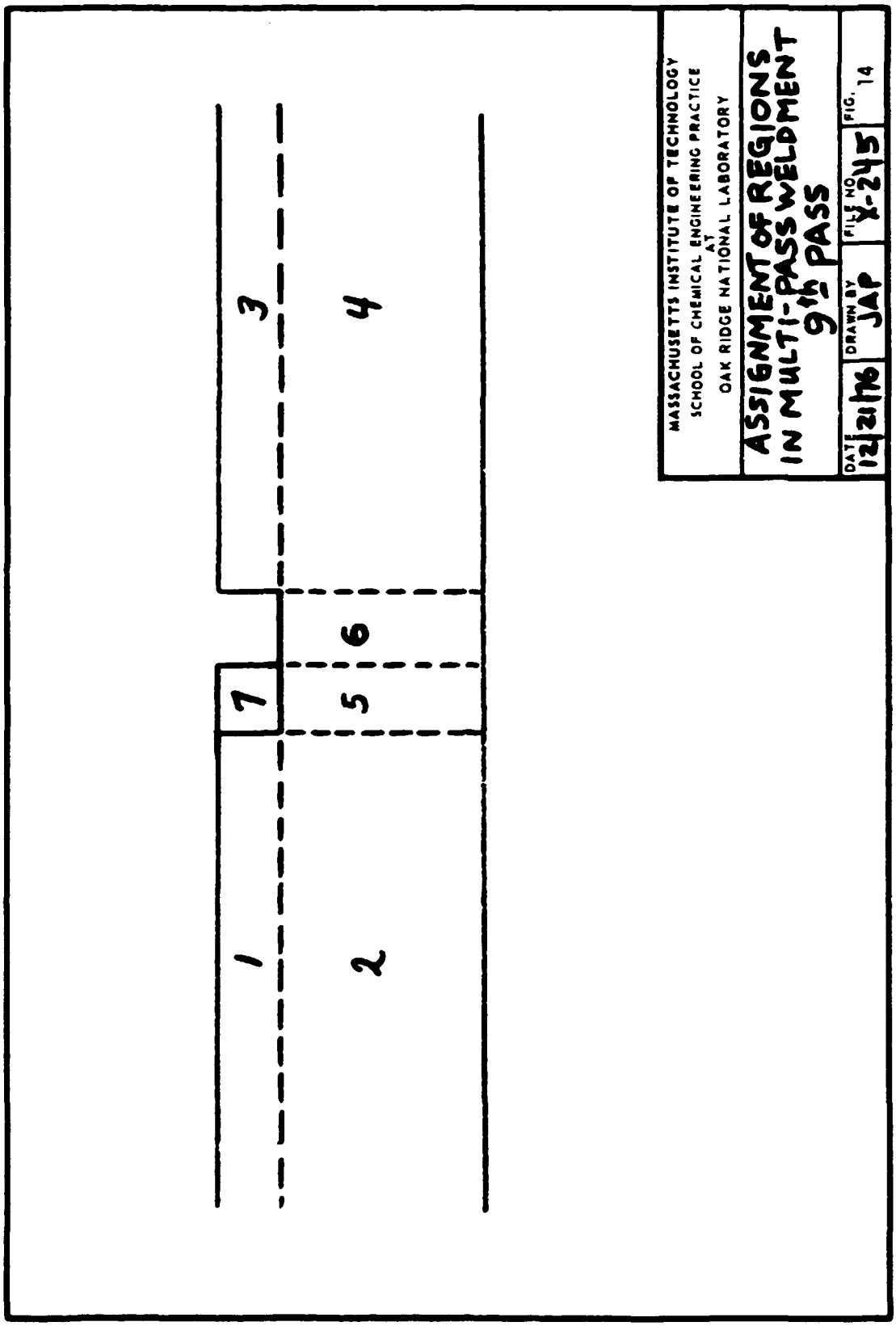
1
2
3
4
5
6
7
MASSACHUSETTS INSTITUTE OF TECHNOLOGY
SCHOOL OF CHEMICAL ENGINEERING PRACTICE
AT
OAK RIDGE NATIONAL LABORATORY
ASSIGNMENT OF REGIONS IN MULTI-PASS WELDMENT 9th PASS
DATE 12/21/76
DRAWN BY JAP
FILE NO. Y-2415
FIG. 14

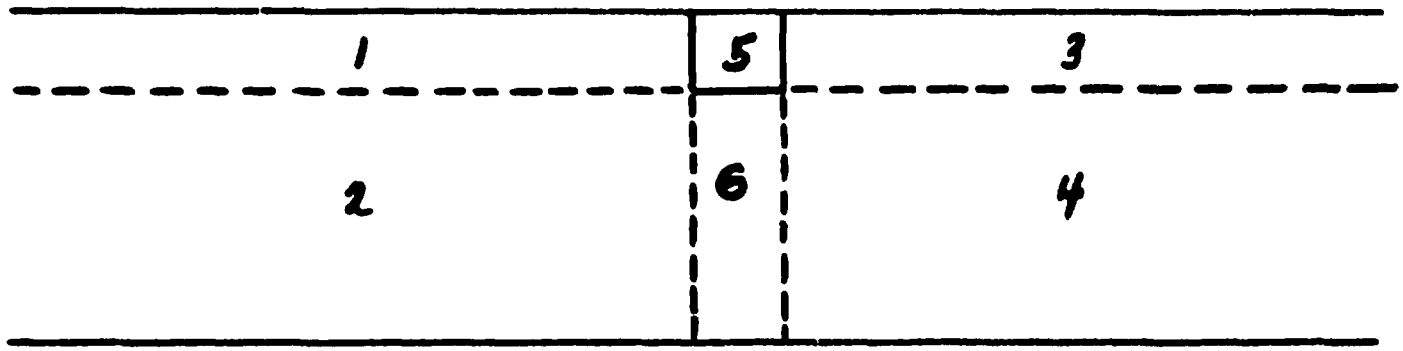

MASSACHUSETTS INSTITUTE OF TECHNOLOGY
SCHOOL OF CHEMICAL ENGINEERING PRACTICE
AT
OAK RIDGE NATIONAL LABORATORY

ASSIGNMENT OF REGIONS IN MULTI-PASS WELDMENT 10th PASS

DATE	DRAWN BY	FILE NO.	FIG.
12/21/76	JAP	X-245	15

It could also compare the peak temperature of each node for the present pass with the temperature of the same node during the previous pass. The higher of the two temperatures would be considered the peak temperature. The alternative to developing routines would be to hand calculate the necessary data. Needless to say, the task would be monumental.

8.2 Sample Calculations

8.2.1 Stability Criteria

From the HEATING5 Manual (16) the solution to the Classical Explicit Program (CEP) will be stable when:

$$\Delta t \leq \left[\frac{C_i}{\sum_{n=1} {}_i K_{\alpha_m}} \right] \text{ minimum for all nodes} \tag{7}$$

C_i is the capacitance of node i. It is calculated from the following equation:

$$C_i = \sum_{\ell=1}^{8} \rho_{i\ell} \, Cp_{i\ell} \, V_\ell \tag{8}$$

where:

$$V_\ell = \left(\frac{\Delta x}{2} \cdot \frac{\Delta y}{2} \cdot \frac{\Delta z}{2}\right)_\ell$$

${}_iK_{\alpha_m}$ is the effective thermal conductance between nodes i and α_m through face m. It is calculated from the following equation.

$$K_{\alpha_m} = \frac{1}{L_m} \sum_{\gamma=1}^{4} k_{m\gamma} A_{m\gamma} \tag{9}$$

where:

$$A_{m\gamma} = \left(\frac{\Delta x}{2} \cdot \frac{\Delta y}{2}\right)\Big|_\gamma \quad \text{for } L_m = \Delta z$$

$$A_{m\gamma} = \left(\frac{\Delta y}{2} \cdot \frac{\Delta z}{2}\right)\Big|_\gamma \quad \text{for } L_m = \Delta x$$

$$A_{mY} = \left(\frac{\Delta x}{2} \cdot \frac{\Delta y}{2}\right)\Big|_{Y} \quad \text{for } L_m = \Delta y$$

To determine whether an interior node or a node with one, two, or three surface faces will be the limiting node, the stability criteria can be applied to an interior node and an imaginary node with six faces exposed to the ambient.

The slab is initialized at T = 121°C throughout so that ρ, C_p, k, h_n, and h_r are constant throughout the slab. If the calculation is simplified by allowing $\Delta x = \Delta y = \Delta z$, then Eq. (8) becomes:

$$C_i = 8\left[\rho C_p\left(\frac{\Delta x^3}{8}\right)\right] = \rho C_p \Delta x^3 \tag{10}$$

Equation (9) becomes:

$$K_{am} = \frac{1}{\Delta x}\left[4\left(k_m \frac{\Delta x^2}{4}\right)\right] = k_m \Delta x \tag{11}$$

Substituting Eqs. (10) and (11) into Eq. (7),

$$\Delta t \leq \frac{\rho C_p \Delta x^3}{6 k_m \Delta x} = \frac{\rho C_p \Delta x^2}{6 k_m} \tag{12}$$

For the hypothetical node with a face exposed to the ambient, the heat transfer coefficient, h, must be related to the effective conductivity, k_{eff}:

$$q_s = h\Delta T \simeq k_{eff} \frac{\Delta T}{\Delta x}$$

Solving for h gives

$$h = \frac{k_{eff}}{\Delta x} \tag{13}$$

Equation (9) then becomes

$$K_{am} = \frac{1}{\Delta x}\left[4(h\Delta x)\frac{\Delta x^2}{4}\right] = h\Delta x^2 \tag{14}$$

for $\Delta y = \Delta z$.

The stability criteria for this node can be evaluated by substituting Eqs. (10) and (14) into Eq. (7).

$$\Delta t \leq \frac{\rho C_p \Delta x^3}{6h\Delta x^2} \equiv \frac{\rho C_p \Delta x}{6h} \tag{15}$$

A comparison between the stable time steps predicted by Eqs. (12) and (15) will determine whether it will be a node located internally or on the edge of the slab which will limit the time step. For stainless steel at 121°C exposed to ambient air at 27°C,

ρ = 7.8 gm/cc

C_p = 0.17 cal/gm-°C

k = 0.075 cal/cm-°C-sec

h_n = 7.54×10^{-5} cal/cm^2-°C-sec, $N_e = \frac{1}{3}$ (horizontal surface, hot side up)

h_r = 6.34×10^{-12} cal/cm^2-°C-sec

h can then be calculated from h_n, N_e, and h_r (T_s and T_a in °K):

$$h = h(T_s^2 + T_a^2)(T_s + T_a) + h_n(T_s - T_a)^{N_e}$$

$$= (6.34\times10^{-12})(394^2 + 300^2)(394 + 300) + (7.54\times10^{-5})(394 - 300)^{1/3}$$

$$= 6.3 \times 10^{-4}$$

Substituting the above properties into Eq. (12) and using Δx = 0.3175 cm, the stable time step for an internal node is calculated.

$$\Delta t \leq \frac{\rho C_p \Delta x^2}{6k} \equiv \frac{(7.8)(0.17)(0.3175)^2}{6(0.075)} = 0.30 \text{ sec}$$

For the imaginary node with six external faces, the stable time step is calculated from Eq. (15) using Δx = 0.3175 cm.

$$\Delta t \leq \frac{\rho C_p \Delta x}{6h} \equiv \frac{(7.8)(0.17)(0.3175)}{6(6.3 \times 10^{-4})} = 111.3 \text{ sec}$$

Hence the largest stable time step will be limited by an interior node.

8.2.2 Calculation of Natural Convection Coefficient

Equation (4) describes the horizontal and vertical natural convection coefficients. Properties for the Gr and Pr numbers for air between 27 - 1600°C are found in Kreith (14). The coefficients are calculated at the average film temperature:

$$T_f = \frac{T_s + T_a}{2}$$

For

$T_s = 121°C$

$T_a = 27°C$

$Pr = 0.72$

$\rho^2 \beta g/\mu^2 = 76.28 \ (°C - cm^3)^{-1}$

$k = 6.9 \times 10^{-5}$ cal/sec-cm-°C

Then

$$Gr = \frac{\rho^2 \beta g \Delta T L^3}{\mu^2} = 76.28 \, L^3 \Delta T$$

For horizontal surfaces (hot side up)

$$h = a \frac{k}{L}(Gr \, Pr)^{Ne} = (0.54)(6.9 \times 10^{-5})[(76.28)(0.72)]^{1/3} \Delta T^{1/3}$$

$$h_n = (0.54)(6.9 \times 10^{-5})[(76.28)(0.72)]^{1/3} = 1.42 \times 10^{-4} \text{ cal/cm}^2\text{-sec-(°C)}^{4/3}$$

For horizontal surfaces (hot side down),

$$h_n = 0.71 \times 10^{-4} \text{ cal/cm}^2\text{-sec-(°C)}^{4/3}$$

For vertical surfaces,

$$h = a\frac{k}{L}(Gr\ Pr)^{N_e} = \frac{(0.14)(6.91\times10^{-5})[(76.28)(0.72)]^{1/4}\ \Delta T^{1/4}}{(1.27)^{1/4}}$$

$$h_n = \frac{(0.14)(6.91\times10^{-5})[(76.28)(0.72)]^{1/4}}{(1.27)^{1/4}}$$

$$= 2.48 \times 10^{-5}\ cal/cm^2\text{-}sec\text{-}(°C)^{5/4}$$

8.2.3 Radiation and Natural Convection Coefficients for Elements on the V-Butt Groove

Since HEATING5 can only handle boundaries which are defined by only one coordinate (such as x = 6), the diagonal boundaries of the wedge were approximated by rectangular regions. To account for the increased surface area exposed to radiation and convection when the diagonal boundary is approximated by rectangles, N_e and h_r were reduced proportional to the difference in areas. For natural convection and radiation from horizontal surfaces, the proportionality factor was calculated as follows:

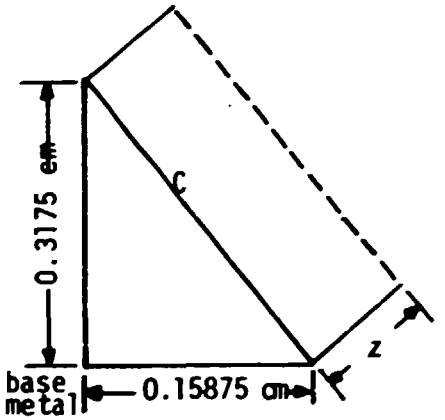

$$C = \sqrt{(0.3175)^2 + (0.15875)^2} = 0.355\ cm$$

$$\frac{\text{actual surface area}}{\text{rectangular surface area}} = \frac{(0.355)z}{[(0.3175) + (0.15875)]z}$$

$$\text{ratio} = 0.745$$

For a surface temperature of 127°C, the actual $h_r = 6.373\times10^{-13}$ cal/°K^4-sec and horizontal $h_n = 7.54\times10^{-5}$ cal/cm^2-°K^4-sec. The coefficients for the wedge can then be calculated as shown.

$$h_{r_{edge}} = 0.745(6.373\times10^{-13}) = 4.748 \times 10^{-13}\ cal/°K^4\text{-}sec$$

$$h_{n_{edge}} = 0.745(7.54\times10^{-5}) = 5.617 \times 10^{-5}\ cal/cm^2\text{-}sec$$

The heat transfer coefficient for vertical surface natural convection is dependent on the length of the heat transfer surface. Since the h_n for vertical convection was entered for a 1.27-cm slab, the h_n for vertical

convection was entered for a 1.27-cm slab, the h_n for vertical convection on the wedge must be recalculated for a length = 0.3175 cm. The ratio is calculated after rearranging the terms in Eq. (4).

$$h = a\,k\,\frac{L^{3/4}}{L}\left(\frac{x}{L^3}\right)^{1/4} \qquad (16)$$

where $x = Gr \cdot Pr$.

$$\frac{h_n \text{ for 0.3175-cm plate}}{h_n \text{ for 1.27-cm plate}} = \frac{(0.3175)^{-1/4}}{(1.27)^{-1/4}} = 1.41$$

The coefficient for vertical convection on the wedge edge is that calculated by correcting for both the actual change in h_n and the additional area due to the approximation of the diagonal line by rectangles. For T_s = 127°C, h_n for vertical convection is 2.22 x 10^{-6} cal/cm^2-°C-sec.

$$h_{n_{edge}} = (0.745)(1.41)(2.22 \times 10^{-6}\ \text{cal/cm}^2\text{-°C-sec})$$
$$= 2.33 \times 10^{-6}\ \text{cal/cm}^2\text{-°C-sec}$$

8.2.4 Effect of Forced Convection

If it is assumed that the argon shield gas flows straight up (perpendicular to the x-z plane) at a rate of 25 ft^3/hr, the velocity of the argon gas flowing past the edges of the weld on the first pass can be calculated:

$$v = \frac{\text{flow area}}{\text{area}}$$

$$= \frac{(25\ \text{ft}^3/\text{hr})(28{,}317\ \text{cc/ft}^3)(1\ \text{hr})}{[2(0.3175)](0.3175)(3600\ \text{sec})} = 975\ \text{cm/sec}$$

From Kreith (7) the forced convection heat transfer coefficient can be calculated with:

$$h_f = \frac{k}{L}(0.0356)\left(\frac{v_0 L}{\alpha}\right)^{0.8}\Big|_{T_{film}} \qquad (17)$$

If argon has the same thermal properties as air, the properties for argon at the two extreme temperatures can be found in Kreith (7). (Shield gas must be less than 1450°C since it is known that forced convection cools the slab. Assume a lower bound of T_{amb} = 27°C.) Equation (17) will then predict h_f:

T_{gas} (°C)	T_{slab} (°C)	T_{film} (°C)	$\alpha)_{film}$ (cm^2/sec)	k Btu/hr-ft-°F	h_f cal/sec-°C-cm^2
27	1470	749	1.68	1.57×10^{-4}	1.142×10^{-3}
1282	1470	1376	3.38	2.11×10^{-4}	8.753×10^{-4}

Hence the highest forced convection flux will be at the lower argon gas temperature.

$$Q_f = h_f A \Delta T = (1.142 \times 10^{-3})[(0.3175)^2(2)](1470 - 27°C)$$

$$= 0.33 \text{ cal/sec} \quad \text{heat lost by forced convection}$$

In comparison, the heat input to the surface under the arc is found from Eq. (1):

$$Q = (0.24)(155)(9.5)(0.40) = 142 \text{ cal/sec}$$

since I = 155 amp, V = 9.5 V, and eff = 0.40. Hence, the total heat lost by forced convection, natural convection and radiation must equal 142 cal/sec. The fraction of the total heat which is lost by forced convection is 0.33/142 = 0.23%

8.3 Location of Data

The entire printout of the computer simulation is in file CEPS-X-245 at the MIT School of Chemical Engineering Practice, Bldg. 3001, ORNL.

8.4 Nomenclature

A surface area, cm^2

a empirically determined constant for dimensionless natural convection formulae, cm^2-°C-sec/cal

$A_{m\gamma}$ $\left(\frac{\Delta x}{2}\right)\left(\frac{\Delta y}{2}\right)\Big|_{\gamma}$ when $L_m = \Delta z$, cm^2

C_p specific heat, cal/gm-°C

C_i capacitance of node i = $\sum_{\ell=1}^{8} \rho_{i\ell} C_{p_{i\ell}} V_\ell$, cal/°C

C length of edge of V-groove for one region, cm

EFF efficiency of welding arc, W added to metal/W generated

Gr Grassoff number $\left(\frac{\rho^2 \beta g \Delta T L^3}{\mu^2}\right)$, dimensionless

g acceleration due to gravity, cm/sec

h combined heat transfer coefficient, cal/sec-cm^2-°C

h_f forced convection heat transfer coefficient, cal/sec-cm^2-°C

h_n natural convection heat transfer coefficient, cal/sec-cm^2-$°C^{he+1}$

h_r radiation heat transfer coefficient, cal/sec-cm^2-$°C^4$

I amperage, amp

k thermal conductivity, cal/sec-cm-°C

k_{eff} effective conductivity in molten pool, cal/sec-cm-°C

K_{am} conductance, $\frac{1}{L_m} \sum_{\gamma=1}^{4} k_{m\gamma} A_{m\gamma}$, cal/sec-°C

L_m Δx, Δy, or Δz, cm

M_i number of faces surrounding a node

N_e exponent for natural convection transfer coefficient, dimensionless

Nu Nusselt number, $h_n L/k$, dimensionless

ℓ indicates solid octant

Pr Prandtl number, $C_p \mu/k$, dimensionless

Q_{arc} heat input to slab from arc, cal/sec-cm^2

Q_{gen} heat generated by arc, cal/sec

Q_f forced convection heat transfer rate, cal/sec

q_s combined heat loss from surface (convection + radiation), cal/sec-cm^2

T temperature, °K

T_a temperature of ambient air, °K

T_f film temperature, °K

T_i initial temperature of slab, °K

T_s temperature of surface of slab, °K

ΔT arithmetic temperature difference ($T_s - T_a$), °K or °C

t time, sec

Δt time step, sec

V voltage, V

V_ℓ 1/8 of elemental volume, $(\frac{\Delta x}{2} \frac{\Delta y}{2} \frac{\Delta z}{2})$, cm^3

v velocity of welding head, cm/sec

v_o argon gas velocity, cm/sec

x coordinate in direction of slab width, cm

y coordinate in direction of slab height, cm

z coordinate in direction of weld filler material, cm

Subscripts

turb in the turbulent zone

melt in the molten laminar flow zone

Greek Symbols

α thermal diffusivity, cm^2/sec

β thermal expansion coefficient, °C^{-1}

ρ density, gm/cc

σ Stephan-Boltzman constant, cal/sec-cm^2-°C^4

μ viscosity, cp

γ indicates planar quadrant

8.5 Literature References

1. Apps, R.L., and D.R. Milner, "A Note on the Behavior of Liquid Metal Under the Arc," Br. Weld. J., 10, 348 (1963).

2. Avdeev, M.V., "Analysis of Hydrodynamic Phenomena in the Weld Pool," Weld. Prod., 10, 1 (1973).

3. British Iron and Steel Research Assn., "Physical Constants of Some Commercial Steels at Elevated Temperatures," Butterworths, London (1953).

4. Grosse, A.R., "Thermal Conductivity of Liquid Metals," U.S. Atomic Energy Commission contract AT(30-1)-2082, Research Institute of Temple University, Philadelphia, Pa. (1964).

5. Hellman, S.K., *et al.*, "Use of Numerical Analysis in Transient Solution of Two-Dimensional Heat Transfer Problem with Natural and Forced Convection, Trans. ASME, 48, 1155 (1956).

6. Kleinschmidt, D.E., *et al.*, "Three-Dimentional Temperature History of a Multipass Filled Weldment, Part 1," ORNL-MIT-241, MIT School of Chemical Engineering Practice, ORNL (October 27, 1976).

7. Kreith, F., "Principles of Heat Transfer," 3rd ed., pp. 81-398, 636, Intext Press, New York (1973).

8. Kublanov, V. Ya, and A.A. Erokhin, "The Arc Force on Molten Metal Pools," Weld. Prod., 5, 11 (1974).

9. Milner, D.R., G.R. Salter, and J.B. Wilkinson, "Arc Characteristics and Their Significance in Welding," Br. Weld J., 7(2), 73 (February 1960).

10. Muraki, T., J.J. Bryan, and K. Masubuchi, "Analysis of Thermal Stresses and Metal Movement During Welding: Part I - Analytical Study," Trans. ASME, J. Eng. Tech., pp. 81-84 (January 1975).

11. Paley, Z., and P.D. Hibbert, "Computation of Temperatures in Actual Weld Design," Weld. J. (Research Supplement), 54(11), 385s (1975).

12. Pavelic, V., R. Tanbakuchi, O.A. Uyehara, and P.S. Myers," Experimental and Computed Temperature Histories in Gas Tungsten-Arc Welding of Thin Plates," Weld. J. (Research Supplement), 48(7), 296s (1969).

13. Perry, R.H., and C.H. Chilton, eds., "Chemical Engineers' Handbook," 5th ed., McGraw-Hill, New York (1973).

14. Rosenthal, D., "The Theory of Moving Sources of Heat and Its Application to Metal Treatments," Trans. ASME, 849 (November 1946).

15. Sarjant, R.J., and M.R. Slack, "Internal Temperature Distribution in the Cooling and Reheating of Steel Ingots," J. Iron Steel Inst., 428 (August 1954).

16. Turner, W.D., and I.I. Siman-Tov, "HEATING5 - An IBM-360 Heat Conduction Program, ORNL-TM-4386 (April 1976).

17. Westby, O., "Temperature Distribution in the Work-Piece by Welding," Univ. of Norway (March 1968).